Journal of Alloys and Compounds 488 (2009) 129–133

Contents lists available at ScienceDirect

Journal of Alloys and Compounds

journal homepage: www.elsevier.com/locate/jallcom

Influence of Mn content on the magnetic properties and microstructure in Fe–Mn–Mo alloys

T. Kırındı*, U. Sarı

Department of Computer Education and Instructional Technology, Kırıkkale University, 71450 Kırıkkale, Turkey

ARTICLE INFO

Article history:
Received 15 July 2009
Received in revised form 31 August 2009
Accepted 1 September 2009
Available online 8 September 2009

Keywords:
Fe–Mn–Mo alloys
Martensitic transformations
Magnetic properties
Electron microscopy
X-ray diffraction
Mössbauer spectroscopy

ABSTRACT

The effects of the Mn content on the magnetic properties and microstructure of the Fe–Mn–Mo alloys have been investigated by means of scanning electron microscopy (SEM), transmission electron microscopy (TEM), X-ray diffraction, and Mössbauer spectroscopy. Experiments reveal that two types of thermal-induced martensites, ε (h.c.p.) and α' (b.c.c.) martensites, form in the as-quenched alloys and these transformations have athermal characters. ε and α' martensites coexist in the Fe–Mn–Mo alloys with 13.4–17.2 wt%Mn content. However, the Mn content affects considerably the amount of martensites and the amount of α' martensite decreases drastically while the amount of ε martensite increases with an increase in Mn content. Furthermore, only ε martensite appears in the case of 20.2 wt%Mn. Mössbauer spectra of the alloys reveal a paramagnetic character with a singlet for the γ (f.c.c.) austenite and ε martensite phases and a ferromagnetic character with a broad sextet for α' martensite phase. With an increase in Mn content, the magnetic character of the Fe–Mn–Mo alloys changes and the ferromagnetic character disappears completely in the case of 20.2 wt%Mn.

© 2009 Elsevier B.V. All rights reserved.

1. Introduction

The martensitic transformations in Fe–Mn alloys have attracted much attention for many years, since they are associated with the unique shape memory, good mechanical properties, and commercial importance [1–4]. The shape memory effect in these alloys related to stress-induced γ (f.c.c.) $\rightarrow$ ε (h.c.p.) martensitic transformation. It is caused by reversion of stress-induced ε martensite on heating [5,6].

In the Fe–Mn alloys, two distinct types of martensite structures, namely ε and α' martensites, might form depending on the Mn content in the austenite γ phase. Martensite formed on cooling is α' below 10 wt%Mn and is ε above 15 wt%Mn. These martensites can also coexist in the alloys with Mn content between 10 and 15 wt% [7,8]. However, both kinds of martensites show different transformation characteristics and physical properties [9–11]. In these alloys, there is a strong relationship between the magnetic behaviour and austenite–martensite phase transformation. The martensitic product phase can exhibit ferromagnetic, antiferromagnetic, and paramagnetic behaviours depending on its type despite the paramagnetic nature of the austenite parent phase. A paramagnetic $\rightarrow$ antiferromagnetic ordering reaction can also occur upon cooling in both the austenite γ and the ε martensite phases of the Fe–Mn alloys, and such a magnetic transition in austenite phase stabilizes γ phase relatively to the competing ε phase [12–14].

The addition of third elements to Fe–Mn alloys influences significantly their several physical properties such as the martensitic transformation, shape memory effect, magnetic behaviours, and mechanical properties. For example, adding small amount of Si improves the shape memory effect [7], while Mo addition increases the strength and hardness of these alloys [3]. Therefore, Fe–Mn–X alloys have attracted much attention. Sarı et al. investigated the influence of Mo on the magnetic properties and martensitic transformation characteristics of a Fe–Mn alloy [2]. Durlu [15,16] studied in detail the forming of the ε martensite in a Fe–Mn–Mo alloy. On the other hand, no satisfactory works have been reported about influence of Mn content in Fe–Mn–Mo alloys. Particularly, the magnetic properties of austenite–martensite transformation in these alloys were not examined sufficiently by Mössbauer spectroscopy technique. The present study focuses on the effect of the Mn content on the magnetic properties and the microstructure of Fe–Mn–Mo alloys. The kinetical, morphological, crystallographic, and magnetic properties of the Fe–Mn–Mo alloys have been investigated by means of SEM, TEM, X-ray diffraction, and Mössbauer spectroscopy.

2. Experimental

The alloys employed in the present study were prepared by vacuum induction melting under an argon atmosphere from pure (99.9%) alloying elements and quenching as cylindrical rods with 1 cm diameter and 10 cm length. Their chemical

* Corresponding author. Tel.: +90 3183572478; fax: +90 3183572487.
E-mail address: talipkirindi@yahoo.com (T. Kırındı).

0925-8388/$ – see front matter © 2009 Elsevier B.V. All rights reserved.
doi:10.1016/j.jallcom.2009.09.004

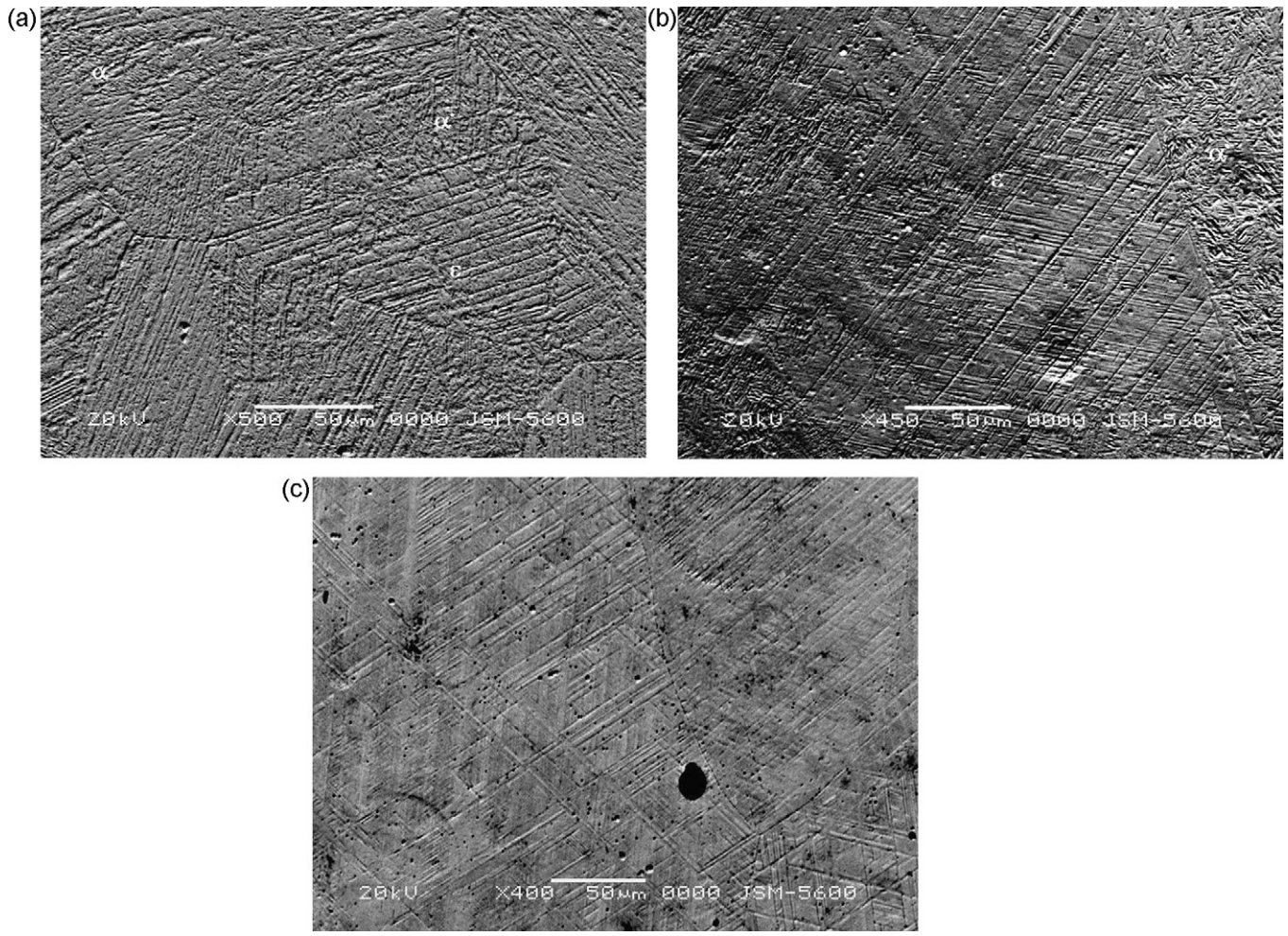

Fig. 1. SEM micrographs showing the microstructure of quenched alloys: (a) Fe–13.4%Mn–5.2%Mo alloy, (b) Fe–17.2%Mn–4.5%Mo alloy and (c) Fe–20.2%Mn–4.8%Mo alloy.

compositions were obtained by using electron dispersion spectroscopy technique (Table 1).

Special slices from the ingot alloys were cut by using diamond saw. Samples were sealed into quartz tubes and then heat treated in the austenite γ-phase equilibrium region. They were homogenized at 1200 °C for 12 h followed by quenching into water at room temperature. For SEM observations, the surfaces of the specimens were first mechanically polished and afterwards the damaged surface layers were eliminated by etching in a solution composed of 5% nitric acid and 95% methanol for 30 s. SEM observations were made in a JEOL 5600 scanning microscope operated at 20 kV.

Samples for TEM observations were prepared from the heat-treated specimens. Discs of about 0.4 mm thick were cut from the samples with a low-speed diamond saw and then thinned to 0.2 mm with 800 and 1200 grit emery papers and punched into 3 mm diameter discs. Finally, these discs were prepared by double jet electropolishing in Streurs-Tenupol jet unit with a solution of 92% acetic acid and 8% perchloric acid at the temperature of 10 °C and a voltage of 20 V. The TEM observations were performed by a JEOL 3010 electron microscope operated at 300 kV with a double tilt specimen. In addition, the volume fraction of α′ and ε martensites were measured by X-ray diffraction method in a Rigaku Geigerflex D-MaxB X-ray diffractometer with Cu Kα radiation and monochromatic.

Mössbauer spectroscopy was applied to study the magnetism and volume fractions of both the austenite and martensite phases. Specimens examined by SEM were used for Mössbauer spectroscopy measurements at room temperature. A spectrometer with a 50 mCi ^{57}Co radioactive source (diffused in Rh) was used during study. A Normos-90 computer program was used to find out the Mössbauer parameters and relative volume fractions of the austenite and martensite phases. The Mössbauer spectra of examined alloys were calibrated with respect to α-Fe and isomer shifts were given relative to the centre of the α-Fe.

Table 1
Chemical composition of the studied alloys (wt%).

Nominal composition	Chemical composition (wt%)		
	Fe	Mn	Mo
Fe–13Mn–5Mo	81.4	13.4	5.2
Fe–17Mn–5Mo	78.3	17.2	4.5
Fe–20Mn–5Mo	75	20.2	4.8

3. Results and discussion

Fig. 1 shows the secondary electron image SEM micrographs of the microstructures forming in the as-quenched alloys. The martensite crystals formed in the grains and austenite grains appear clearly in the alloys. It indicates that the martensitic transformation starting temperatures (M_s) of the alloys is higher than the room temperature. The martensite plates have different morphologies in austenite grains. The figures show obviously that ε and α′ martensites coexist in the Fe–Mn–Mo alloys with 13.4 and 17.2 wt%Mn contents (Fig. 1a and b), whereas only ε martensite exists in the case of 20.2 wt%Mn (Fig. 1c). While the ε martensite plates appear generally as parallel stacks of fine bands, the α′ martensites form as little particles in thin plates tangle [1,6]. Most of the bands of ε martensite pass through the whole grain, i.e., from one end of grain boundary to the other, and the surface relief is composed of many parallel scratches (Fig. 1). In addition, microstructure observations reveal that the transformations in the alloys have athermal characteristic. In this type transformation, the nucleation of the martensite phases is generally considered as heterogeneous [17]. Nishiyama and Kajiwara found that

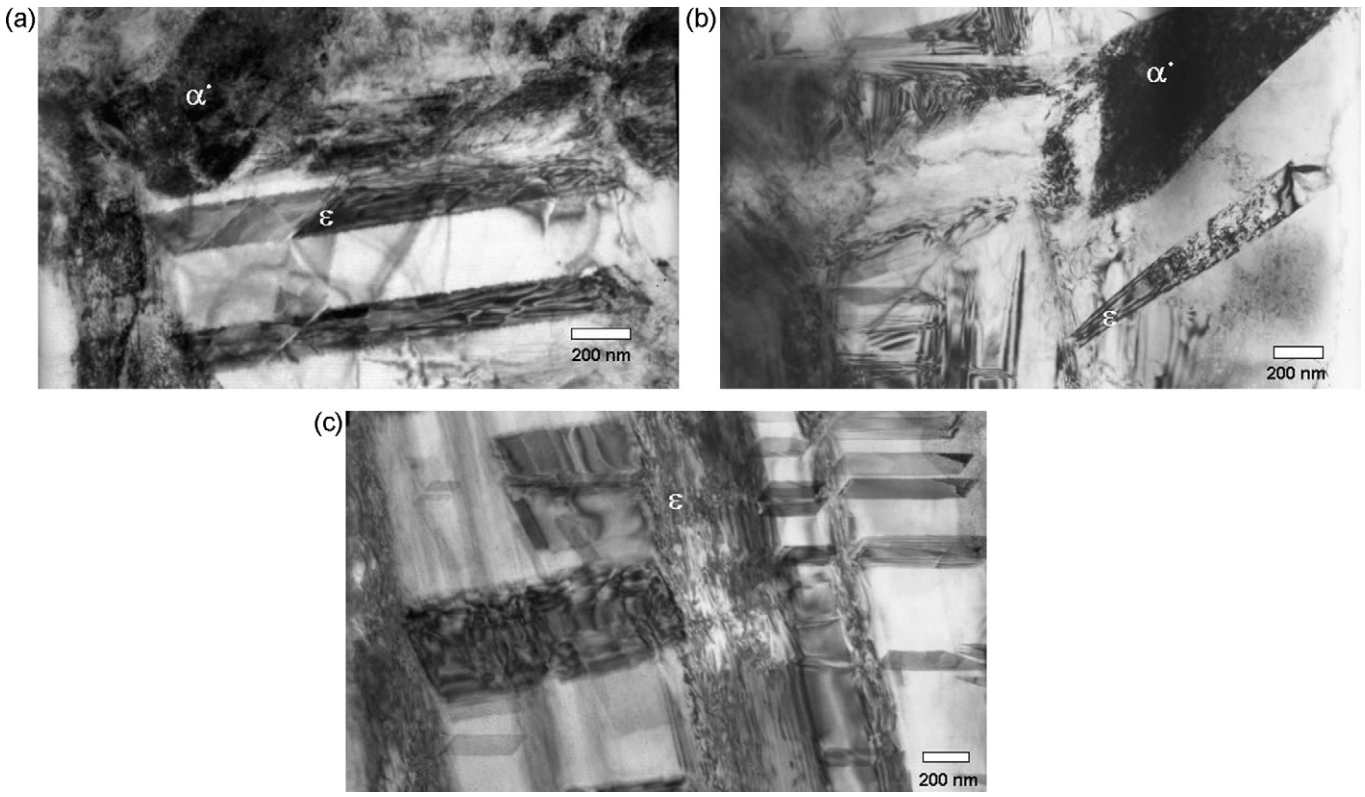

Fig. 2. TEM images of alloys: (a) Fe–13.4%Mn–5.2%Mo alloy, (b) Fe–17.2%Mn–4.5%Mo alloy and (c) Fe–20.2%Mn–4.8%Mo alloy.

further isothermal holding times cause either new nucleation sites or the growth of prior martensite crystals in the same specimen for some ferrous alloys [9,18]. To check out this well-known information, quenched alloys were subsequently kept in water at room temperature for 30 min and these specimens were investigated by SEM again. Later observations revealed the absence of isothermal martensite crystals.

Fig. 2 shows the TEM bright field images of quenched alloys at room temperature. Here the ε and α' martensite plates are seen clearly in the alloys. On the other hand, only ε martensite appears in the Fe–20.2%Mn–4.8%Mo alloy (Fig. 2c) In addition, the stacking faults appear obviously in austenite phase (Fig. 2b and c). They create embryos for the ε martensite formation. The models describing ε martensite formation were based on the assumption of overlapping stacking faults on every second close-packed plane of the austenite phase and the transformation occurs with the movement $a/6\langle 1\,1\,2\rangle$ Shockley partial dislocations [15,16]. The formation of the α' martensite crystals has been established to be mainly associated with dislocations in prior austenite phase and they appear dislocated austenite areas [9,19].

The amount of ε and α' martensites occurred in the alloys was also evaluated by X-ray diffraction method. Fig. 3 shows X-ray diffraction patterns of the alloys. The figure indicates clearly that the intensities of ε martensite peaks increase while the intensities of α' martensite peaks decrease with increasing Mn contents. The peak of $\alpha'(2\,0\,0)$is clearly seen for Fe–13.4%Mn–5.2%Mo and Fe–17.2%Mn–4.5%Mo alloys whereas it disappear in the case of Fe–20.2%Mn–4.8%Mo. Only ε martensite and austenite γ peaks appear in this case. The results of X-ray experiments agree that SEM and TEM observations well.

The magnetic characters of the austenite and martensite phases have been examined with Mössbauer spectroscopy technique. Fig. 4 shows the Mössbauer spectra obtained at room temperature on the

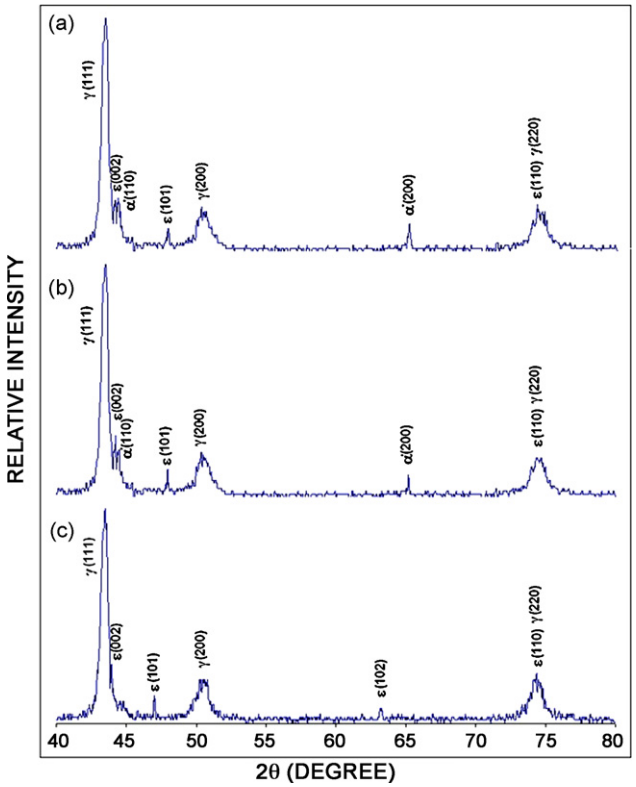

Fig. 3. X-ray diffraction patterns of the alloys: (a) Fe–13.4%Mn–5.2%Mo alloy, (b) Fe–17.2%Mn–4.5%Mo alloy and (c) Fe–20.2%Mn–4.8%Mo alloy.

Table 2
Some Mössbauer parameters of the alloys.

Alloys (wt%)	γ + ε phase (%)	α′ phase (%)	$\delta_{\gamma+\varepsilon} \pm 0.002$ (mm/s)	$\delta_{\alpha'} \pm 0.001$ (mm/s)	B_{hf} (α′) (Tesla)
Fe–13.4Mn–5.2Mo	28.136	71.864	−0.2379	−0.1104	30.54
Fe–17.2Mn–4.5Mo	74.816	25.184	−0.247	-0.086	30.59
Fe–20.2Mn–4.8Mo	100	–	−0.233	–	–

quenched alloys. Spectra are characterized by a broad sextet and a central singlet in the alloys with 13.4 and 17.2 wt%Mn contents while only singlet exists in Fe-20.2%Mn–4.8%Mo alloy. As is well known, in Mössbauer spectroscopy, ferromagnetic (or antiferromagnetic) character of materials displays a typical sextet whereas paramagnetic structure exhibits only a singlet. Besides, α′ (b.c.c.) phase is a ferromagnetic while γ (f.c.c.) and ε (h.c.p.) phases display generally paramagnetic character in Fe–Mn alloys [20–22]. Therefore, in Fig. 4, the sextets belong to ferromagnetic α′ martensite phase as the paramagnetic singlets can be ascribed either to γ austenite phase or to ε martensite phase. The results show that paramagnetic → ferromagnetic transition occurs also along with γ → α′ martensitic transformation in the alloys. In addition, Fig. 4 exhibits that ferromagnetic sextet area decreases as Mn content increases and it entirely disappears in the case of 20.2%Mn. Thus, the ferromagnetic character of the Fe–Mn–Mo alloys gradually disappears. It stem from changing of martensite structure. Ferromagnetic α′ martensite phase vanishes and only ε martensite phase, which has paramagnetic character, occurs in the Fe–Mn–Mo alloy with high Mn content.

The Mössbauer parameters such as isomer shifts (δ), hyperfine magnetic fields (B_{hf}) with the calculated % volume fractions of phases are given in Table 2. It is almost impossible to sort the paramagnetic γ and ε phases out by Mössbauer spectrometry at room temperature [23]. Therefore, the volume fractions of ε and γ phases are evaluated together in Table 2. According to Mössbauer results, the volume fractions of γ, ε and α′ phases change with Mn content in the alloys (Fig. 5). While the amount of ε martensite increases, the amount of α′ martensite decreases significantly with increasing Mn content (Fig. 5 and Table 2). On the other hand, the Mn content does not influences considerably internal magnetic field in the Fe–Mn–Mo with 13.4 and 17.2 wt%Mn contents while the magnetic field disappear in Fe–20.2%Mn–4.8%Mo alloy (Table 2).

In Fe–Mn alloys, studies on the austenite → martensite phase transformations have revealed that austenite γ phase can be transformed to ε and α′ martensites, and ε → α′ transformation is also possible under some physical conditions. The γ → ε → α′ transformation can be induced by plastic deformation. This transformation behaviour is quite sensitive to the Mn content of alloy [8,9]. Our results show that the Mn content affects considerably the type of martensite in Fe–Mn–Mo alloys. Martensite formed on cooling is α′ (b.c.c.) and ε (h.c.p.) in 13.4–17.2 wt%Mn alloy and is ε in a high 20.2%Mn alloy. Thus, it can be said that increasing of Mn content in Fe–Mn–Mo alloys stabilizes the ε martensite with respect to α′ martensite. According to Maji and Krishnan [24], the formation of α′ martensite is responsible for incomplete recover and acts by impeding reverse motion of the Shockley partial dislocations. Therefore, shape memory effect of the alloy can be increased with an increase in Mn content.

This study shows that the martensitic transformation behaviour in Fe–Mn–Mo alloys is quite sensitive to the Mn content of alloy just as in Fe–Mn alloys. With an increase in the Mn content, the amount of ε martensite increases while the amount of α′ martensite decreases, and the α′ martensite completely disappears in the case of 20.2%Mn alloy with high Mn content. On the other hand, the amount of α′ martensite increases in the case of low Mn content and it can expected that only α′ martensite appears in the case of less than 10%Mn as in Fe–Mn alloys [7–9]. Thus, the ferromagnetic character along with smaller paramagnetic austenite appears for lower Mn concentration.

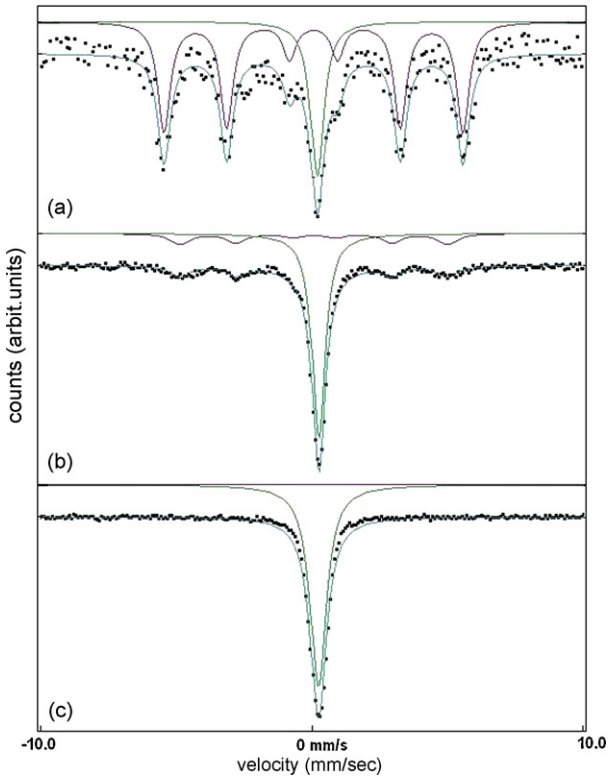

Fig. 4. Room temperature Mössbauer spectra for quenched alloys: (a) Fe–13.4%Mn–5.2%Mo alloy, (b) Fe–17.2%Mn–4.5%Mo alloy and (c) Fe–20.2% Mn–4.8%Mo alloy.

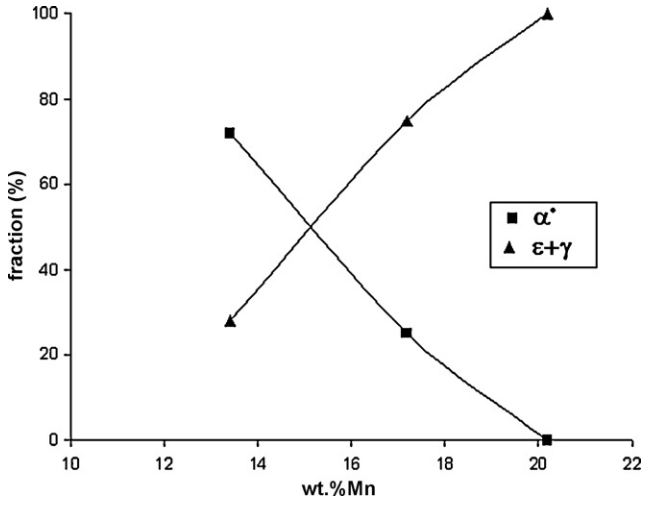

Fig. 5. Volume fractures of occurred phase for the alloys used in this work as a function of Mn content.

4. Conclusions

In this paper, the effects of the Mn content on the magnetic properties and microstructure in Fe–Mn–Mo alloys were investigated and the results were summarized as follows:

1. Experiments reveal that two types of thermal-induced martensites, ε and α' martensites, form in the Fe–Mn–Mo alloys and these transformations exhibit athermal characters. The Mn content in Fe–Mn–Mo alloys affects type of martensite. ε and α' martensites coexist in the case of 13.4–17.2 wt%Mn contents, while only ε martensite exists in the case of high Mn content.
2. With an increase in the Mn content, the volume fractions of the phases change and the amount of α' martensite decreases significantly while the amount of ε martensite increases. The increasing Mn content stabilizes the ε martensite with respect to α' martensite.
3. The Mössbauer spectra of the alloys show that the α' martensite phase has a ferromagnetic character whereas the γ austenite and ε martensite phases display a paramagnetic character. The spectra reveal that paramagnetic $\rightarrow$ ferromagnetic transition occur along with $\gamma \rightarrow \alpha$' martensitic transformation in the alloys. The magnetic character of the Fe–Mn–Mo alloy change with Mn content. The ferromagnetic character disappears as Mn content increases due to changing of martensite structure with high Mn content.

Acknowledgements

This study was supported by the Kırıkkale University Scientific Research Fund with the project numbers 2008/34 and 2008/35.

References

[1] T. Kirindi, E. Güler, M. Dikici, J. Alloy Compd. 433 (2007) 202–206.
[2] U. Sarı, T. Kırındı, M. Yüksel, S. Ağan, J. Alloy Compd. 476 (2009) 160–163.
[3] T.N. Durlu, J. Mater. Sci. Lett. 16 (1997) 320–321.
[4] J.H. Jun, C.S. Choi, Mater. Sci. Eng. A A252 (1991) 133–138.
[5] T. Kirindi, M. Dikici, J. Alloy Compd. 407 (2006) 157–162.
[6] T. Kırındı, U. Sarı, M. Dikici, J. Alloy Compd. 475 (2009) 145–150.
[7] S. Cotes, A.F. Guillermet, M. Sade, J. Alloy Compd. 278 (1998) 231–238.
[8] L. Xing, Q. Zuoxiang, Z. Yansheng, W. Xingyu, L. Fengxian, D. Bingzhe, H. Zhuangqi, J. Mater. Sci. 35 (2000) 5597–5603.
[9] Z. Nishiyama, Martensitic Transformation, Academic Press, London, 1978.
[10] J. Martinez, S.M. Cotes, A.F. Cabrera, J. Desimoni, A.F. Guillermet, Mater. Sci. Eng. A 408 (2005) 26–32.
[11] M. Acet, T. Schneider, B. Gehrmann, E.F. Wassermann, J. Phys. IV 5 (1995) 379–384.
[12] P. Marinelli, A.F. Guillermet, M. Sade, Mater. Sci. Eng. A 373 (2004) 1–9.
[13] O.A. Khomenko, I.F. Khilkevic, G.Y. Zvigintseva, Phys. Met. Metallogr. 37 (1974) 186–191.
[14] S. Cotes, M. Sade, A.F. Guillermet, Metal. Mater. Trans. A 26 (1995) 1957–1969.
[15] T.N. Durlu, J. Mater. Sci. 34 (1999) 2887–2890.
[16] T.N. Durlu, J. Mater. Sci. Lett. 15 (1996) 2134–2136.
[17] S.M. Cotes, A.F. Guillermet, M. Sade, Metal. Mater. Trans. A 35 (2004) 83–91.
[18] S. Kajiwara, Acta Metall. 32 (1984) 407–413.
[19] E. Güler, T. Kirindi, H. Aktaş, J. Alloy Compd. 440 (2007) 168–172.
[20] J.H. Yang, H. Chen, C.M. Wayman, Metall. Trans. A 23 (1992) 1439–1444.
[21] M. Mizrahi, A.F. Cabrera, S.M. Cotes, S.J. Stewart, R.C. Mercader, J. Desimoni, Hyperfine Interact. 156/157 (2004) 541–545.
[22] S.M. Cotes, A.F. Cabrera, L.C. Damonte, R.C. Mercader, J. Desimoni, Hyperfine Interact. 141/142 (2002) 409–414.
[23] S.M. Cotes, A.F. Cabrera, L.C. Damonte, R.C. Mercader, J. Desimoni, Physica B 320 (2002) 274–277.
[24] B.C. Maji, M. Krishnan, Scripta Mater. 48 (2003) 71–77.